

Comparison between the Classes Method and the Quadrature Method of Moments for multiphase systems

Original

Comparison between the Classes Method and the Quadrature Method of Moments for multiphase systems / Marchisio, Daniele; Barresi, Antonello; Baldi, Giancarlo; Fox, R. O.. - STAMPA. - (2002), pp. 283-300. (Intervento presentato al convegno 8th International Conference on Multiphase Flows in Industrial plants tenutosi a Alba (CN, Italy) nel 18-20 September 2002).

Availability:

This version is available at: 11583/1408266 since: 2016-09-18T00:21:59Z

Publisher:

ANIMP Servizi srl

Published

DOI:

Terms of use:

openAccess

This article is made available under terms and conditions as specified in the corresponding bibliographic description in the repository

Publisher copyright

(Article begins on next page)

ANIMP
Multiphase Flow
Engineering
Section

POLITECNICO OF TURIN
Department of Material
Science and Chemical
Engineering

AIDIC
Italian Association
of Chemical
Engineering



AIDIC



Proceedings

Eighth International Conference

**Multiphase Flow in
Industrial Plants**

Palazzo delle Mostre e dei Congressi
Alba, Cuneo, Italy
September 18-19-20, 2002

COMPARISON BETWEEN THE CLASSES METHOD AND
THE QUADRATURE METHOD OF MOMENTS FOR MULTIPHASE SYSTEMS

D.L. Marchisio, A.A. Barresi, G. Baldi and R.O. Fox

283-300

ANIMP

Italian Association of Industrial Plant Engineering

Via Spalato 11/2 – 20124 Milan – Italy

Ph. +39 (2) 6070242

Fax +39 (2) 6070245

e-mail: anna@animp.it

Casa Editrice

ANIMP Servizi Srl

Via Spalato 11/2 – 20124 Milan – Italy

Pubblicazione realizzata da:

ELIO TICINESE PICKING PACK SERVICE POINT Srl

Via Venosa, 4/6 – 20137 Milan – Italy

ISBN

88-88198-03-02

COMPARISON BETWEEN THE CLASSES METHOD AND THE QUADRATURE METHOD OF MOMENTS FOR MULTIPHASE SYSTEMS

D.L. Marchisio¹, A.A. Barresi, G. Baldi

Dipartimento di Scienza dei Materiali ed Ingegneria Chimica

Politecnico di Torino, Torino, Italia

and R.O. Fox

Department of Chemical Engineering

Iowa State University, Ames, IA, USA

Abstract

Investigation of multiphase systems generally requires the solution of the population balance equation; bubble columns, crystallisation and precipitation reactors are some examples of important industrial applications. As mixing also plays an important role in determining phase interactions, often the population balance has to be included in a Computational Fluid Dynamics (CFD) code. This can be accomplished only if the source term is provided in an adequate way. Several methods have been proposed; one of the most popular is the Discretised Population Balance (DPB) which presents the disadvantage of requiring an elevate number of scalars to be solved, leading to high computation times. A promising alternative is the Quadrature Method of Moment (QMOM) in which the population balance is written in terms of the transport equation of the moments of the number density function, and all the integrals involving this function are solved through an ad-hoc quadrature approximation. The method has been validated and extended to breakage in previous works, while in this work its performance is compared with those of a DPB approach. The comparison is made in terms of accuracy of prediction, computational time and simplicity of implementation in a CFD code.

¹ Corresponding author: marchis@iastate.edu; current affiliation: Dept. of Chem. Eng., Iowa State University, 3131 Sweeney Hall, Ames (IA) 50011-2230, USA

1. Introduction

The solution of the population balance equation by using Moment Methods (MMs) has been first proposed by Hulburt and Katz [1]. In their work they highlighted the promising possibilities but also the strong limitations of the method. MMs are based on the solution of the population balance equation through the moments of the Particle Size Distribution (PSD). Thus if $n(L; \mathbf{x}, t)$ is the PSD in terms of the particle length L , the k^{th} moments of the PSD is defined as follows:

$$m_k(\mathbf{x}, t) = \int_0^{+\infty} n(L; \mathbf{x}, t) L^k dL.$$

The main advantage of this method stands in the possibility of defining the PSD only by tracking a few lower-order moments. However, the method is not suitable when modelling size-dependent molecular growth, and size-dependent aggregation and breakage.

Different methods have been proposed in order to solve the closure problem raised by Hulburt and Katz and the subject is extensively discussed in [2]. One of the most promising is the QMOM that was first proposed by McGraw [3] for studying aerosol evolution. The method is based on the solution of the integrals involving the PSD through a quadrature approximation:

$$m_k(\mathbf{x}, t) = \int_0^{+\infty} n(L; \mathbf{x}, t) L^k dL \approx \sum_{j=1}^N w_j L_j^k$$

where abscissas L_j and weights w_j are calculated from the lower-order moments by using the Product-Difference (PD) algorithm [4].

The method has been validated in the case of molecular growth and aggregation through comparison with analytical solutions and Monte Carlo simulations [5] and compared with other available approaches, such as Laguerre quadrature approximation and the finite element method, for the solution of the aerosol general dynamic equation [6]. Moreover, lately the QMOM has been extended to the description of bivariate population balances [7, 8], where the PSD is written in terms of more than one internal coordinate (e.g., particle volume and surface area). The QMOM can be also used for modelling breakage and extension and validation of the model for this case can be found in [9]. The aim of this work is to compare its performances with those of a Classes Method.

2. The Quadrature Method of Moments

The Reynolds averaged transport equation of the k^{th} moment is as follows:

$$\frac{\partial m_k(\mathbf{x}, t)}{\partial t} + \langle u_i \rangle \frac{\partial m_k(\mathbf{x}, t)}{\partial x_i} - \frac{\partial}{\partial x_i} \left[\Gamma_t \frac{\partial m_k(\mathbf{x}, t)}{\partial x_i} \right] = S_k(\mathbf{x}, t)$$

where $\langle u_i \rangle$ is the Reynolds-averaged velocity in the i^{th} direction, Γ_t is the turbulent diffusivity, and the source term is

$$S_k(\mathbf{x}, t) = (0)^k J(\mathbf{x}, t) + \int_0^{+\infty} k L^{k-1} G(L) n(L; \mathbf{x}, t) dL + \overline{B}_k(\mathbf{x}, t) - \overline{D}_k(\mathbf{x}, t)$$

In this expression, $J(\mathbf{x}, t)$ is the nucleation rate, $G(L)$ is the molecular growth rate, and $\overline{B}_k(\mathbf{x}, t)$ and $\overline{D}_k(\mathbf{x}, t)$ are the birth and death term due to aggregation and breakage, that can be expressed as follows:

$$\begin{aligned} \overline{B}_k(\mathbf{x}, t) &= \frac{1}{2} \int_0^{+\infty} n(\lambda; \mathbf{x}, t) \int_0^{+\infty} \beta(u, \lambda) (u^3 + \lambda^3)^{k/3} n(u; \mathbf{x}, t) du d\lambda \\ &\quad + \int_0^{+\infty} L^k \int_0^{+\infty} a(\lambda) b(L|\lambda) n(\lambda; \mathbf{x}, t) d\lambda dL \end{aligned}$$

and

$$\begin{aligned} \overline{D}_k(\mathbf{x}, t) &= \int_0^{+\infty} L^k n(L; \mathbf{x}, t) \int_0^{+\infty} \beta(L, \lambda) n(\lambda; \mathbf{x}, t) d\lambda dL \\ &\quad + \int_0^{+\infty} L^k a(L) n(L; \mathbf{x}, t) dL \end{aligned}$$

where $\beta(u, \lambda)$ is the aggregation kernel, $a(\lambda)$ is the breakage kernel, and $b(L|\lambda)$ is the fragment distribution function.

When the QMOM is used, all the integral terms included in the above equations are calculated through a quadrature approximation leading to

$$S_k(\mathbf{x}, t) = (0)^k J(\mathbf{x}, t) + \sum_{j=1}^N k L_j^{k-1} G(L_j) w_j + \frac{1}{2} \sum_{i=1}^N w_i \sum_{j=1}^N w_j (L_i^3 + L_j^3)^{k/3} \beta_{ij} \\ + \sum_{i=1}^N a_i \bar{b}_i^{(k)} w_i - \sum_{i=1}^N L_i^k w_i \sum_{j=1}^N w_j \beta_{ij} - \sum_{i=1}^N L_i^k a_i w_i,$$

where $\beta_{ij} = \beta(L_i, L_j)$, $a_i = a(L_i)$ and

$$\bar{b}_i^{(k)} = \int_0^{+\infty} L^k b(L|L_i) dL.$$

The number of nodes N used in the quadrature approximation determines the number of moments to be tracked. In fact, in order to calculate a quadrature approximation of order N , the first $2N$ moments have to be calculated. For example if $N=2$ then $k=(0, \dots, 3)$ or if $N=3$ then $k=(0, \dots, 5)$ or if $N=4$ thus $k=(0, \dots, 7)$.

The role of this parameter on the model performance has been already investigated in a previous work [9], and a quadrature approximation with three nodes ($N=3$) was found to be a good trade off between accuracy and computational costs.

3. Classes methods: the Hounslow's approach

A number of discretised population balances (DPBs) or classes methods (CMs) have been proposed for simultaneous modelling of nucleation, growth and aggregation and breakage; recently Vanni [10] reviewed and compared a wide variety of zero-order CMs.

Here we consider the method proposed by Hounslow and co-workers [11]. Hounslow's approach is based on the idea that aggregates are formed of particles of 2^{j-1} monomers (as if only particles composed 1, 2, 4, 8, ... monomers exist). As already mentioned, by using this method the internal coordinate is discretised, and thus in terms of length-based expressions, it becomes $L_{i+1} = L_i 2^{1/3}$.

In the original formulation the discretisation was fixed and the model was proposed only for molecular growth and aggregation. The model is derived by defining 4 binary interaction mechanisms that produce a birth or a death in the i^{th} interval. Aggregation between a particle in the $(i-1)^{\text{th}}$ and of a particle in the first to $(i-2)^{\text{th}}$ interval produces a new particle in the i^{th} interval. Aggregation between two particles both in the $(i-1)^{\text{th}}$ interval results in the formation of a particle in the i^{th} interval. Death occurs to a particle in the i^{th}

interval should it aggregate with a particle of sufficient size for the resultant aggregate to be larger than the upper size limit of the i^{th} interval. If a particle in the i^{th} interval aggregates with a particle from that or a higher interval, a death occurs in the i^{th} interval.

The final model consists of the following set of transport equations:

$$\frac{\partial N_i(\mathbf{x}, t)}{\partial t} + \langle u_i \rangle \frac{\partial N_i(\mathbf{x}, t)}{\partial x_i} - \frac{\partial}{\partial x_i} \left[\Gamma_i \frac{\partial N_i(\mathbf{x}, t)}{\partial x_i} \right] = S_i(\mathbf{x}, t)$$

where

$$\begin{aligned} S_i(\mathbf{x}, t) = & \frac{2}{(1+r)L_m} \left(\frac{r}{r^2-1} G(L_{i-1}) N_{i-1} + G(L_i) N_i - \frac{r}{r^2-1} G(L_{i+1}) N_{i+1} \right) \\ & + N_{i-1} \sum_{m=1}^{i-1} 2^{m-i+1} \beta_{i-1,m} N_m + \frac{1}{2} \beta_{i-1,m-1} N_{i-1}^2 \\ & - N_i \sum_{m=1}^{i-1} 2^{m-i} \beta_{i,m} N_m - N_i \sum_{m=i}^{\infty} \beta_{i,m} N_m \end{aligned}$$

where N_i is the population of the class of particles of size L_i and $r = L_{i+1}/L_i$. From the function N_i , it is possible to derive the moments of the PSD by using the following expression:

$$m_k(\mathbf{x}, t) = \sum_{i=1}^C \overline{L_i^k} N_i(\mathbf{x}, t)$$

where $\overline{L_i^k}$ is the appropriate mean size and C is the total number of classes.

It is interesting to notice here that differently from the QMOM, using a CM the PSD is known but generally only two of the moments of the PSD can be tracked correctly [usually $k=0$ (total particle number density) and $k=3$ (total particle volume)], whereas using the QMOM all the tracked moments are known with very small errors [5,6,9]. In this formulation of the model the total number of classes C has to be chosen (with L_0), in order to cover the entire range of particle length.

More recently, a revised version of the model has been proposed [12] using an adjustable discretised population balance, by means of a parameter q , and thus the discretisation scheme becomes:

$$L_{i+1} = L_i (2^{1/q})^{1/3}.$$

This modified version of the original model has been also extended to breakage problems [10] and in this case the total number of classes is $C \cdot q$. Hounslow's approach gives quite good performances in the case of aggregation with simultaneous nucleation and growth. Other methods exist, but give good performances only in the case of purely aggregation, or purely nucleation and growth.

In general, in order to work with good accuracy, an elevated number of classes is needed (e.g., 20-30 for simple problems, and 100-200 for complex problems) and as already mentioned for CFD applications this would result in an enormous amount of calculations, since this elevated number of transport equations has to be solved in every cell of the computational domain.

4. Operating conditions and computational details

As already mentioned, simulations using the DPB for modelling the solid evolution is computationally expensive, whereas the QMOM proposed here presents the main advantage of requiring much less computational resources; however both approaches must be coupled with CFD codes. By using CFD every cell of the computational domain can be seen as a perfectly mixed reactor that exchanges mass and energy with the surrounding cells because of mean velocities and turbulent diffusion. Since both the approaches are linked with the CFD code, use of one of the two affects model predictions locally.

The aim of this work is the investigation of this local difference of accuracy. Both simulations are carried out in a simple fluid dynamic system: the perfectly mixed reactor (i.e., a single cell of the computational domain). In this ideal reactor no spatial macro-gradients exist, and therefore the properties of the system are constant throughout the domain.

The QMOM has been already validated through comparison with analytical solutions and Monte Carlo simulations, leading to the conclusion that three nodes are sufficient to track the first six moments (m_0, \dots, m_5) with very small errors [5]. For this reason in what follows the QMOM will be considered the exact solution of the problem.

The implementation of the models requires the solution of a system of ordinary differential equations (ODE) and the solution of the eigenvalues problem. The first one was solved by using the ODE package ODEPACK (LSODE Fortran double precision subroutine), whereas for the second one the linear algebra package EISPACK (IMTQL2 Fortran double precision subroutine) was used.

In this work only aggregation is considered, and the comparison is carried out in three different conditions:

1. Constant kernel $\beta(L, \lambda) = \beta_0$
2. Brownian kernel $\beta(L, \lambda) = \beta_0 \frac{(L + \lambda)^2}{L\lambda}$
3. Hydrodynamic kernel $\beta(L, \lambda) = \beta_0 (L + \lambda)^3$

The three cases were tested with different initial PSDs and here results for monomodal and a bimodal initial PSDs are presented.

5. Results and discussion

The monomodal PSD is shown in Fig. 1 and in the same figure is also reported the PSD at different time steps after aggregation with constant kernel ($\beta_0 = 10^{-17} \text{ m}^3/\text{s}$) by using the DPB proposed by Hounslow. As it is possible to see aggregation causes the disappearance of smaller particles to form bigger particles. The evolution of the moments is reported in Fig. 2. Results clearly show that m_3 remains constant, since during aggregation total particle volume is conserved. The moments of order lower than three decrease whereas the others increase.

In order to quantify the ability of the model to predict system properties it is useful to define the intensity of aggregation [13].

$$I_{agg} = 1 - \frac{m_0(t)}{m_0(t=0)}.$$

I_{agg} is 0 when the number of aggregation events is null and goes to 1 as this number increases. In the case under investigation (constant kernel) the QMOM was proved to predict moment evolutions with errors lower than 0.01% [5]. For this reason the QMOM will be considered as exact solution, and the DPB predictions will be compared. From the comparison an error of 4% was detected when I_{agg} is equal to 0.95. In Fig. 3 the error committed by using DPB (assuming the prediction of the QMOM to be exact) is reported against I_{agg} . As it is possible to see the error on moments of order lower than three is less than 2%, whereas the third moment is perfectly predicted.

For moments of order greater than three the error is still less than 10% for I_{agg} close to one. Note that in normal crystallisation/precipitation reactors I_{agg} typically falls in the range between 0.5-0.6, where the errors are lower.

The behaviour of the bimodal PSD in case of aggregation with constant kernel is shown in Fig. 4. In Fig. 5 the percentage errors for the first six moments are reported. As it is possible to see the situation is slightly different, in fact the error on m_0 is quite high and when I_{agg} is equal to 0.5 becomes stable at about 10%. All the other moments behave in a similar way, but the errors are greater than for the monomodal case.

The previous results are obtained by using 20 classes; only after adopting the modification proposed by Lister [12] with $q=5$ the prediction is as good as the QMOM. Thus for equivalent accuracy, the QMOM requires six scalars while the DPB requires 100 for the constant kernel case.

In the case of Brownian aggregation, the PSD at different time steps is reported in Fig. 6 using the same initial conditions, but with $\beta_0 = 2.5 \cdot 10^{-18} \text{ m}^3/\text{s}$. This different value of β_0 was used in order to have comparable values of I_{agg} . As it is possible to see, the evolution is slightly different, especially for smaller particles that seem to aggregate faster. The errors (always calculated assuming the QMOM to be exact) are of the same order of magnitude of the previous case (see Fig. 7). Moreover, results confirm that in this case (and generally for the monomodal distribution) the case of Brownian aggregation can be treated with constant kernel: in fact, under the hypothesis of aggregating particles of the same size

$$\beta(L, \lambda) = \beta_0 \frac{(L + \lambda)^2}{L\lambda} \approx 4\beta_0$$

For the bimodal distribution, results are very similar. In Fig. 8 the PSD at different time steps is reported. Again in this case smaller particles aggregate faster, but their weight on the final mean crystal size is small. Also in this case the error in m_0 is quite high, but remains lower than 10% until $I_{agg} < 0.5$ (see Fig. 9).

In the case of hydrodynamic kernel, the same initial conditions were used with $\beta_0 = 1.5 \cdot 10^6 \text{ m}^3/\text{s}$. This value of β_0 was used in order to obtain comparable values of I_{agg} . The evolution of the PSD predicted by the DPB is reported in Fig. 10. As it is possible to note, the tail of the PSD increases faster with time as a proof of the increased ability of bigger particles to collide and aggregate. In this case agreement between the two models is not as good as in the previous cases. However, it is useful to highlight that

for moderate aggregation rates ($I_{agg} < 0.5$) errors are around 10-15% (see Fig. 11). The presented results were obtained using 30 classes. Comparison with the QMOM showed that only using $q=5$ are the errors of the same order of magnitude as QMOM for the hydrodynamic kernel.

In Fig. 12 the PSD at different time steps, in the case of initial bimodal distribution for the hydrodynamic kernel, is reported. Note that in this case in order to obtain the same range of I_{agg} a different β_o was used ($\beta_o = 5.0 \cdot 10^4 \text{ m}^3/\text{s}$). Up to $I_{agg} < 0.25$ all the errors are lower than 10%, but for I_{agg} close to one the m_4 error goes up to 800% (see Fig. 13).

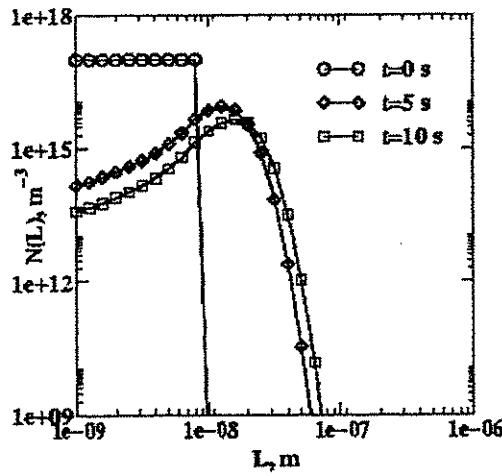


Fig. 1. Aggregation with constant kernel ($\beta_o = 10^{-17} \text{ m}^3/\text{s}$): PSD at different time steps calculated with the DPB approach.

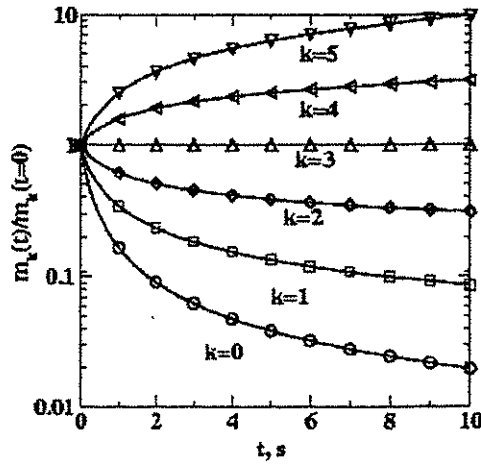


Fig. 2. Aggregation with constant kernel ($\beta_0 = 10^{-17} \text{ m}^3/\text{s}$): time evolution of the normalized moments of the PSD predicted by the DPB.

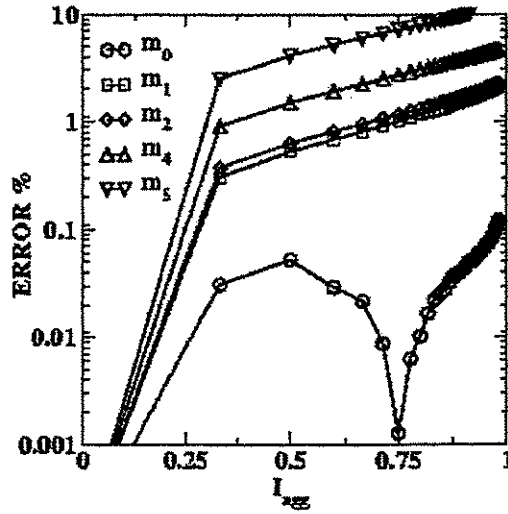


Fig. 3. Aggregation with constant kernel ($\beta_0 = 10^{-17} \text{ m}^3/\text{s}$): percent errors of the first six moments calculated with the DPB (m_3 is not reported since the error is lower than $10^{-5}\%$).

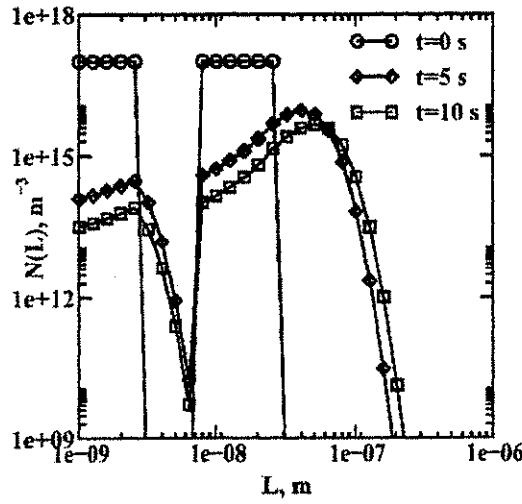


Fig. 4. Aggregation with constant kernel ($\beta_o = 10^{-17} \text{ m}^3/\text{s}$): PSD at different time steps calculated with the DPB approach.

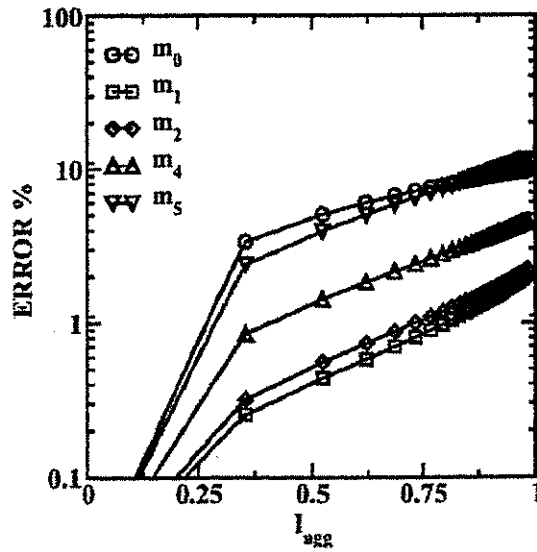


Fig. 5. Aggregation with constant kernel ($\beta_o = 10^{-17} \text{ m}^3/\text{s}$): percent errors of the first six moments calculated with the DPB (m_3 is not reported since the error is lower than $10^{-5}\%$).

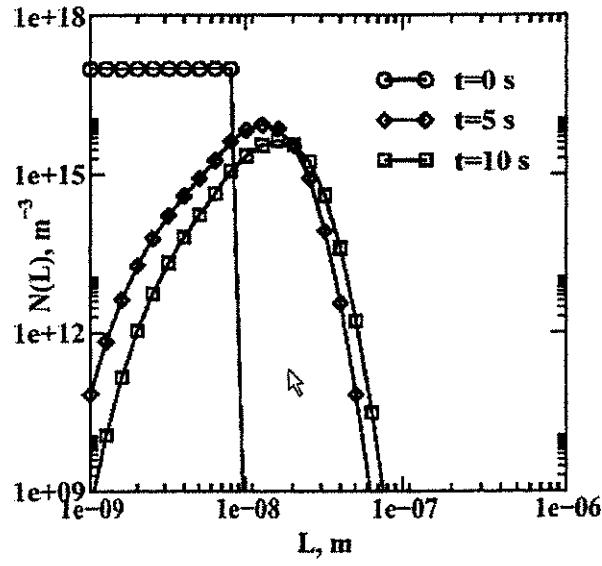


Fig. 6. Aggregation with Brownian kernel ($\beta_o = 2.5 \cdot 10^{-18} \text{ m}^3/\text{s}$): PSD at different time steps calculated with the DPB approach.

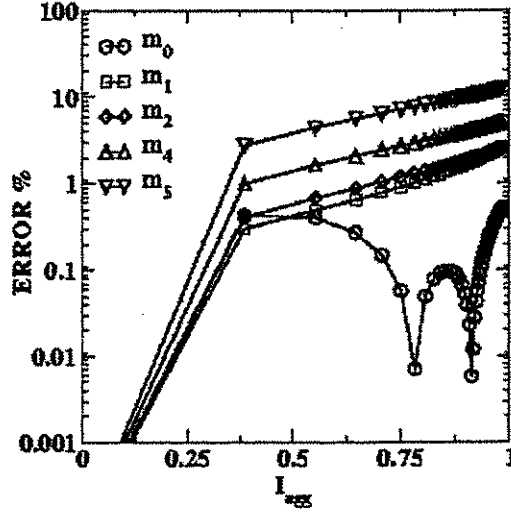


Fig. 7. Aggregation with Brownian kernel ($\beta_o = 2.5 \cdot 10^{-18} \text{ m}^3/\text{s}$): percent errors of the first six moments calculated with the DPB (m_3 is not reported since the error is lower than $10^{-5}\%$).

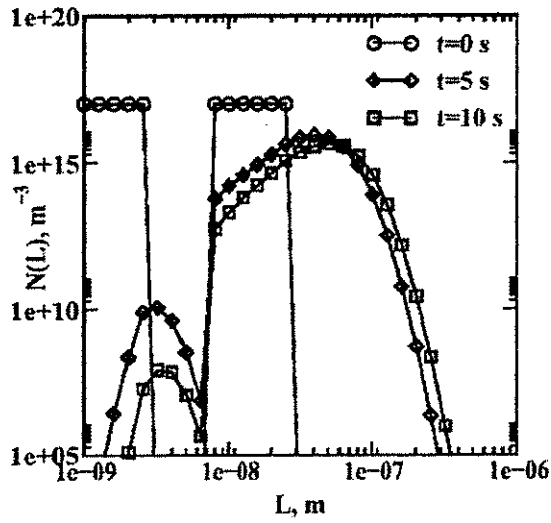


Fig. 8. Aggregation with Brownian kernel ($\beta_o = 2.5 \cdot 10^{-18} \text{ m}^3/\text{s}$): PSD at different time steps calculated with the DPB approach.

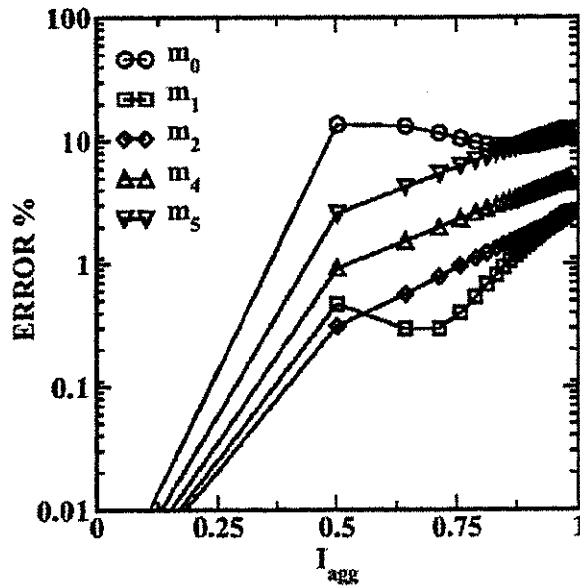


Fig. 9. Aggregation with Brownian kernel ($\beta_o = 2.5 \cdot 10^{-18} \text{ m}^3/\text{s}$): percent errors of the first six moments calculated with the DPB (m_3 is not reported since the error is lower than $10^{-5}\%$).

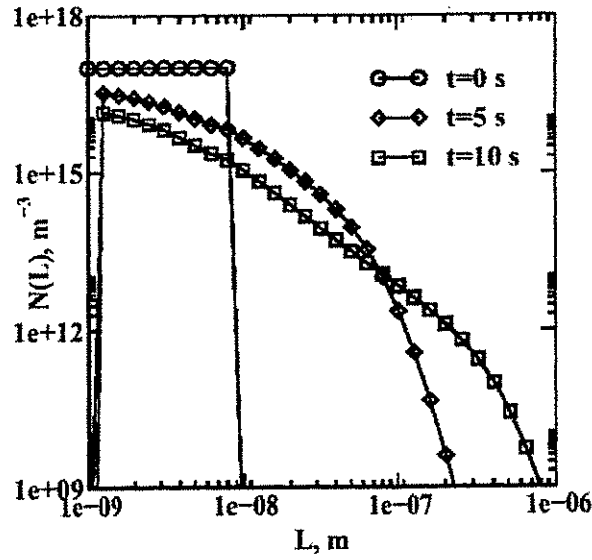


Fig. 10. Aggregation with hydrodynamic kernel ($\beta_o = 1.5 \cdot 10^6$ 1/s): PSD at different time steps calculated with the DPB approach.

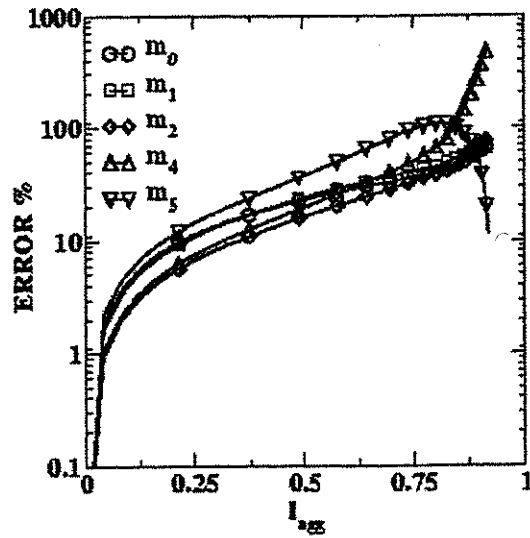


Fig. 11. Aggregation with hydrodynamic kernel ($\beta_o = 1.5 \cdot 10^6$ 1/s): percent errors of the first six moments calculated with the DPB (m_3 is not reported since the error is lower than $10^{-5}\%$).

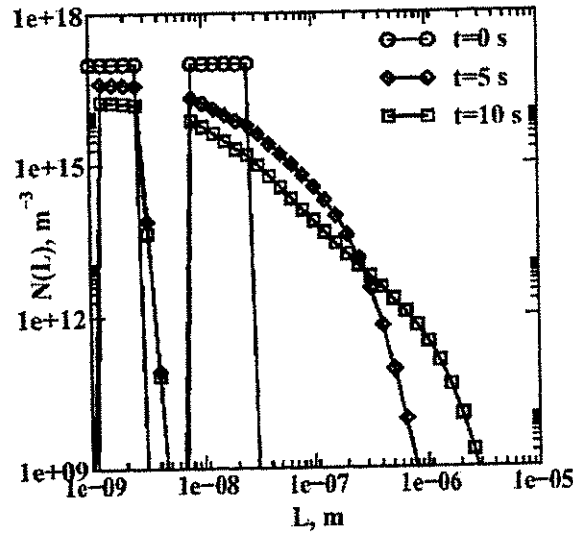


Fig. 12. Aggregation with hydrodynamic kernel ($\beta_o = 5.4 \cdot 10^4$ 1/s): PSD at different time steps calculated with the DPB approach.

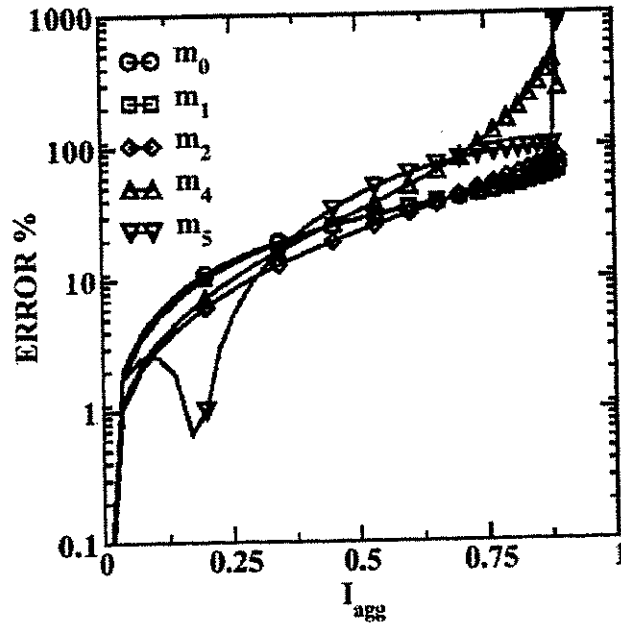


Fig. 13. Aggregation with hydrodynamic kernel ($\beta_o = 5.4 \cdot 10^4$ 1/s): percent errors of the first six moments calculated with the DPB (m_3 is not reported since the error is lower than $10^{-5}\%$).

6. Conclusions and further developments

The comparisons presented above lead us to the conclusion that in the case of constant or Brownian kernel, the DPB proposed by Hounslow in the original formulation ($q=1$) works quite well by tracking only 15-20 classes, but in order to have errors as low as the QMOM, 75-100 classes have to be used.

Nevertheless, even for this simple case some limitations were detected. For example, the model performance in the case of initial bimodal PSD was worse than with a monomodal PSD.

The DPB used in this work can be applied also in case of hydrodynamic aggregation for moderate aggregation rates, but in order to predict the moments with the same accuracy of the QMOM, the number of classes has to be increased at least to 150.

The comparison between the QMOM and the DPB proposed by Hounslow showed that the QMOM method is indeed fascinating for several reasons. The method is very fast, in fact the reduction of the number of scalars to be tracked is drastic (from 50-100 to 6) and in general does not depend on the width of the PSD. This reduction of scalars has a strong impact on CPU time, in fact by using the QMOM method a reduction of 150-200 times was detected with respect to the DPB. In addition, as mentioned before, the QMOM does not present the problem of fixing the intervals to be considered in the simulations. Thus, unlike the DPB approach, it can be used without any modification for different PSDs.

The QMOM has been already implemented in a commercial CFD code for modelling aggregation-breakage problems in solid-liquid systems [14] and its applications can be easily extended to other practical cases, such as solid-gas, gas-liquid and liquid-liquid systems. The currently available treatment for the bivariate case [7,8] has an implicit formulation that requires an optimisation procedure for its solution and seems to be too heavy for CFD applications. For this reason we are currently working on an explicit formulation of the problem (Direct Quadrature Method of Moments) that will be reported in a future communication [15].

Acknowledgements - The research has been partially supported by an Italian National research project (PRIN – Analysis and modelling of solid-liquid mixing processes).

Notation

a	breakage kernel
b	fragment distribution function
B_k	birth rate
C	total number of classes
D_k	death rate
G	molecular growth rate
I_{agg}	intensity of aggregation
J	nucleation rate
L	particle length
L_j	abscissa of quadrature approximation
m_k	kth moment of the PSD
n	PSD in term of the particle length
N	number of modes in quadrature approximation
N_i	population of the class
q	Hounslow's parameter
S_k	source term
t	time
$\langle u_i \rangle$	Reynolds-averaged velocity
w_j	weight of quadrature approximation
\mathbf{x}	coordinate vector
β	aggregation kernel
Γ_t	turbulent diffusivity

References

- [1] Hulburt, H.M. and Katz, S., Chem. Eng. Sci., 19, p.555, 1964.
- [2] Diemer, R.B. and Olson, J.H., Chem. Eng. Sci., to appear, 2002.
- [3] McGraw, R., Aer. Sci. Tech., 27, p. 255, 1997.
- [4] Gordon, R.G., J. Math. Phys., 9, p. 655, 1968.
- [5] Marchisio, D.L., Piktuna, J.T., Fox, R.O., Vigil, D.R. and Barresi, A.A., AIChE J., submitted, 2002.
- [6] Barret, J.C. and Webb, N.A., J. Aerosol Sci., 29, p. 31, 1998.

- [7] Wright, D.L., McGraw, R. and Rosner, D.E., J. Colloid Interface Sci., 236, p. 242, 2001.
- [8] Rosner, D.E. and Pyykonen, J.J., AIChE J., 48, p. 476, 2002.
- [9] Marchisio, D.L., Vigil, D.R. and Fox, R.O., J. Colloid Interface Sci., submitted, 2002.
- [10] Vanni, M., J. Colloid Interface Sci., 221, p.143, 2000.
- [11] Hounslow, M.J., Ryall, R.L., and Marshall, V.R., AIChE J., 34, p. 1821, 1988.
- [12] Lister, J.D., Smit, D.J., and Hounslow, M.J., AIChE J., 41, p. 591, 1995.
- [13] Ilievski, D., and Hounslow, M.J., AIChE J., 41, p. 525, 1995.
- [14] Marchisio, D.L., Pikturna, J., Wang, L., Vigil, R.D., and Fox, R.O.: "Use of the Quadrature Method of Moments for modelling population balances in CFD applications". Proceedings 15th International Symposium on Industrial Crystallization, Sorrento, Italia, 2002.
- [15] Marchisio, D.L. and Fox, R.O.: "A Direct Quadrature Approximation for population balances". Annual meeting of the American Institute of Chemical Engineers, Indianapolis, IN, USA, 2002.

SCIENTIFIC COMMITTEE

Giancarlo Baldi
Politecnico di Torino
Ugo Billardo
Università "La Sapienza", Roma
Gian Piero Celata
Enea Casaccia, Roma
Giorgio Donsì
Università di Salerno
Dario Ercolani
Snamprogetti S.p.A., Centro di Fano
Sergio Fabbri
Università di Bologna
Giovanna Ferrari
Università di Salerno
Brunello Formisani
Università della Calabria
Francesco Ferrini
Techfem S.r.l., Fano
Giancarlo Giacchetta
Università di Ancona
Giovanni Guglielmini
Università di Genova
Carlo Lombardi
Politecnico di Milano
Barbara Mazzarotta
Università "La Sapienza", Roma
Agostino Mazzoni
ENI S.p.A. - Div. AGIP, Milano
Arrigo Pareschi
Università di Bologna
Cesare Saccani
Università di Bologna
Alessandro Terenzi
Snamprogetti S.p.A., Centro di Fano
Marco Vanni
Politecnico di Torino

ORGANIZING COMMITTEE

Giancarlo Baldi
Politecnico di Torino
Augusto Bianchini
Università di Bologna
Marco Bravi
Università di Roma
Marco Fossa
Università di Genova

Organizing Secretariat of the Conference
Anna Valenti, ANIMP, Milano